



Measurement of the Michel Parameters in Leptonic Tau Decays using the OPAL Detector at LEP

R. Bartoldus ^{a*}

^a Physikalisches Institut, Universität Bonn, Nußallee 12, D-53115 Bonn, Germany
e-mail: Rainer.Bartoldus@cern.ch

A measurement of the Michel parameters in τ decays is presented [1] which involves a novel method to fit the energy spectra and energy-energy correlations of the charged decay leptons from τ -pair events produced in e^+e^- collisions close to $\sqrt{s} = m_{Z^0}$. The parameters ρ_ℓ , ξ_ℓ , $(\xi\delta)_\ell$ (with $\ell = e, \mu$) and η_μ have been extracted from a global likelihood fit of Monte Carlo generated events to the data set recorded with the OPAL detector in the years 1990–1995. If e - μ universality is assumed and inferring the τ polarization from neutral current data, the measured Michel parameters are $\rho = 0.781 \pm 0.028 \pm 0.018$, $\xi = 0.98 \pm 0.22 \pm 0.10$, $\xi\delta = 0.65 \pm 0.14 \pm 0.07$ and $\eta = 0.027 \pm 0.055 \pm 0.005$, where the value of η has been constrained using the published OPAL measurements of the leptonic branching ratios and the τ lifetime. Limits on the masses of new intermediate bosons and on non-standard couplings are obtained. It is explained how such limits can be derived from an investigation of the Michel parameter space.

1. INTRODUCTION

1.1. Lorentz structure

In the Standard Model (SM) the charged weak interaction is described by the exchange of left-handed W bosons, i.e., by a pure vector coupling to only left-handed fermions. Thus, in the low-energy four-fermion ansatz, the Lorentz structure of the charged current is predicted to be of the type V–A. Deviations from this behavior would indicate new physics and might be caused by changes in the W-boson couplings or through interactions mediated by new gauge bosons [2]. Many such extensions involving heavy new bosons are likely to emerge first in the decay of the massive τ lepton. Among all its decay modes, the decays $\tau \rightarrow e\nu_e\nu_\tau$ and $\tau \rightarrow \mu\nu_\mu\nu_\tau$ are the only ones in which the electroweak couplings can be probed without disturbance from the strong interaction. The purely leptonic τ decays represent therefore an ideal system to study the Lorentz structure of the charged weak current.

The most general, derivative-free, four-lepton interaction matrix element for the $\tau \rightarrow \ell\nu_\ell\nu_\tau$ decay that is local and Lorentz invariant can be

written as:

$$\mathcal{M} = 4 \frac{G_0}{\sqrt{2}} \sum_{\substack{\gamma=S,V,T \\ \epsilon,\omega=R,L}} g_{\epsilon\omega}^\gamma \langle \bar{\ell}_\epsilon | \Gamma^\gamma | \nu_\ell \rangle \langle \bar{\nu}_\tau | \Gamma_\gamma | \tau_\omega \rangle. \quad (1)$$

Here γ denotes the type of interaction (scalar, vector or tensor) with Γ^γ being defined in terms of the Dirac matrices, $\Gamma^S = 1$, $\Gamma^V = \gamma^\mu$, $\Gamma^T = \frac{1}{\sqrt{2}} \sigma^{\mu\nu}$. The indices ω and ϵ denote the chiralities of the τ lepton and its charged decay lepton, ℓ , respectively. The matrix element involves 10 complex coupling constants, $g_{\epsilon\omega}^\gamma$, for which the SM predicts $g_{LL}^V=1$ and all others being zero. One usually normalizes the sum of their absolute squares such that $|g^S| \leq 2$, $|g^V| \leq 1$ and $|g^T| \leq \frac{1}{\sqrt{3}}$. The total strength can be incorporated into G_0 which then accounts for deviations from the Fermi constant G_F .

1.2. Michel parameters

After integration over the unobserved neutrino momenta and the spin of the charged decay lepton, only four different combinations of these coupling constants, denoted by ρ , ξ , $\xi\delta$ and η , determine the shape of the decay spectra. Neglecting radiative corrections, neutrino masses and terms proportional to $(\frac{m_\ell}{m_\tau})^2$, the leptonic decay width

*now The University of Iowa, c/o SLAC, P.O. Box 4349, MS 59, Stanford, CA 94309, USA

can, after boosting into the Z^0 rest frame, be written as:

$$\begin{aligned} \frac{d\Gamma_\ell}{dx} = \frac{G_0^2 m_\tau^5}{192\pi^3} & \left\{ (2 - 6x^2 + 4x^3) \right. \\ & + \frac{4}{3} \rho_\ell \left(-\frac{1}{3} + 3x^2 - \frac{8}{3}x^3 \right) \\ & + 12 \eta_\ell \frac{m_\ell}{m_\tau} (1 - 2x + x^2) \\ & - P_\tau \left[\xi_\ell \left(-\frac{2}{3} + 4x - 6x^2 + \frac{8}{3}x^3 \right) \right. \\ & \left. \left. + \frac{4}{3} (\xi\delta)_\ell \left(\frac{1}{3} - 4x + 9x^2 - \frac{16}{3}x^3 \right) \right] \right\}. \end{aligned} \quad (2)$$

Here $x = E_\ell/E_\ell^{\max}$ is the scaled energy of the charged decay lepton with $E_\ell^{\max} \approx E_\tau$ being its maximal energy. P_τ is the average τ polarization. Each spectrum is described by four Michel parameters [3, 4] for which the SM predicts the values $\rho = \frac{3}{4}$, $\xi = 1$, $\xi\delta = \frac{3}{4}$ and $\eta = 0$ according to a V–A structure of the charged weak current. Because the η_ℓ -term is suppressed by a factor $\frac{m_\ell}{m_\tau}$, there is almost no sensitivity to η_e , which is therefore set to zero. This leaves the 7 parameters ρ_e , ξ_e , $(\xi\delta)_e$, and ρ_μ , ξ_μ , $(\xi\delta)_\mu$, η_μ to be determined.

At LEP, τ pairs are produced with almost perfect spin correlation.² For parallel τ spins the correlation function between two leptonic decays in the event can be written as [5, 6]:

$$\begin{aligned} I(x_1, x_2) = & f(x_1)f(x_2) + g(x_1)g(x_2) \\ & - P_\tau [f(x_1)g(x_2) + f(x_2)g(x_1)], \end{aligned} \quad (3)$$

where $f(x; \rho, \eta)$ and $g(x; \xi, \xi\delta)$ include the above third-order polynomials. In contrast to uncorrelated single decay spectra here the product of the two spin-dependent parts, $g(x_1)g(x_2)$, appears without the suppression by the τ polarization. It thus provides high sensitivity to the parameters ξ and $\xi\delta$.

1.3. Tau polarization

In principle, it is desirable to treat the neutral current (Z^0 couplings) in the same generality as the charged current. This would, however, increase the number of free parameters to

²For V and A type couplings in the production, the τ^+ and τ^- have opposite chiralities.

an amount that cannot be handled given the statistical significance of the available lepton spectra. For this reason previous experiments have already restricted to only V and A type couplings in the τ production when fitting the τ polarization along with the Michel parameters. For the present analysis this small gain in generality does not justify the loss in precision due to additional correlations between the parameters. Therefore, the τ polarization has been inferred from an independent fit to neutral current data using the ZFITTER package.³ As input to the calculation of P_τ the following values were used [7]: $m_{Z^0} = (91.1884 \pm 0.0022)$ GeV, $m_t = (175 \pm 6)$ GeV, $m_{H^0} = 300$ GeV with $60 \text{ GeV} < m_{H^0} < 1 \text{ TeV}$, $\alpha_s(m_{Z^0}) = 0.118 \pm 0.003$ and $\alpha(m_{Z^0})^{-1} = 128.90 \pm 0.09$. These values yield the τ polarization at the Z^0 peak as $P_\tau = -0.1391^{+0.0069}_{-0.0055}$, where the dominant uncertainty is due to the unknown Higgs boson mass.

In this analysis, data taken at $\sqrt{s} = m_{Z^0}$ are used together with data below and above m_{Z^0} . Averaging accordingly over the energy dependence of P_τ yields the same quoted value. This leads to an uncertainty in P_τ of approximately 5% which is still smaller than the error of the current direct measurements (e.g. [8]).

2. EVENT SELECTION

2.1. Tau pair selection

From the data set of 155 pb^{-1} integrated luminosity collected with the OPAL detector [9], τ -pair events are selected following the strategy described in earlier publications [8]. First, lepton pairs are preselected by requiring exactly two charged jet-cones of 35° half-opening angle with low track and cluster multiplicity. Two-photon events are rejected by requiring either a large visible energy or an unbalanced transverse momentum sum, and a small acollinearity.

From this sample Bhabha events are removed based on a large sum of cluster energies or a large sum of track momenta in conjunction with large cluster energies. After that, μ -pair events are

³Note that since all direct measurements of P_τ have implicitly assumed a V–A structure in the decay they would introduce a bias if used as input for the fit.

eliminated if consistent with high track momenta, small energy deposit in the calorimeter or signals in the muon chambers. The remaining 147 042 events are almost entirely τ pairs. The geometrical acceptance of this selection covers the region $|\cos\theta| < 0.95$.

2.2. Tau decay mode identification

A likelihood selection is used to identify the τ -decay modes in the two cones. It distinguishes between the 1-prong decays $\tau \rightarrow e \nu_e \nu_\tau$, $\tau \rightarrow \mu \nu_\mu \nu_\tau$ and $\tau \rightarrow h \nu_\tau$ where h is either π , ρ or $a_1 \rightarrow \pi 2\pi^0$.⁴ It makes use of a set of variables which allow the discrimination of different channels.

These variables include: the ratio of the energy deposited in the electromagnetic calorimeter (ECAL) and the track momentum measured in the central detector, E/p , the specific energy loss in the jet chamber, dE/dx , the fraction of ECAL energy in the cone that is not associated to the track, the number of hits in the last 3 HCAL layers and in the 4 layers of the muon chambers and the matching probability between the extrapolated track and a muon chamber track segment. The measured variables are compared to simulated reference distributions for the considered decay modes. To obtain high purity samples, the cones involving the lepton are required to be identified with a relative likelihood of $P > 90\%$.

As observables for the fit, the track momentum of the muon measured in the jet chamber, and the energy deposited by the electron in the ECAL, are used, both scaled to the beam energy.

2.3. Selection efficiency and Background

Based on the decays of both τ leptons, the events are divided into mutually exclusive samples of single-lepton decays (e-h, μ -h) and lepton-lepton correlations (e- μ).

The e-e and μ - μ samples are subject to a large background contamination from Bhabha and μ -pair events as well as from two-photon events, $\gamma\gamma \rightarrow e^+e^-$ and $\gamma\gamma \rightarrow \mu^+\mu^-$, which distort the correlation spectra in the two most sensitive regions, where both leptons have high energies or both have low energies, respectively. To avoid a

dominating systematic uncertainty in the estimation of these backgrounds, the e-e and μ - μ event classes are excluded from the fit.

After additional geometrical cuts on the individual samples, that exclude insensitive or inadequately simulated regions of the detector, the efficiencies quoted in table 1 are obtained.

	Event class		
	e-h	μ -h	e- μ
Sample size	19369	21190	5834
Efficiency	83.1%	88.6%	85.8%

Table 1
Selection efficiencies for the three event classes.

Among various background sources the main contribution comes from the misidentification of hadronic τ decays. In addition, Bhabha and μ -pair events pass the selection, when, e.g., in an $e^+e^- \rightarrow e^+e^-$ event one electron is misidentified as $\tau \rightarrow \rho \nu_\tau$ decay, or in an $e^+e^- \rightarrow \mu^+\mu^-$ event one muon fakes a $\tau \rightarrow \pi \nu_\tau$ decay. Table 2 lists all significant backgrounds in the three event samples.

3. FITTING METHOD

3.1. Basis spectra

Since the single decay amplitudes depend linearly on the Michel parameters, it is possible to decompose any observed spectrum into different basis spectra with each representing a specific set of parameters. To describe the entire parameter space, five spectra have to be mixed with coefficients that add up to unity. A basis has to be chosen with Michel parameter sets that are both physically meaningful and sufficiently uncorrelated. Among several equivalent choices, the one used is:

$$\begin{pmatrix} \rho_n \\ \xi_n \\ \xi\delta_n \\ \eta_n \end{pmatrix} = \begin{pmatrix} 3/4 \\ 1 \\ 3/4 \\ 0 \end{pmatrix}, \begin{pmatrix} 1 \\ 0 \\ 0 \\ 0 \end{pmatrix}, \begin{pmatrix} 0 \\ 1 \\ 0 \\ 0 \end{pmatrix}, \begin{pmatrix} 3/4 \\ 0 \\ 0 \\ 1/2 \end{pmatrix}, \begin{pmatrix} 0 \\ 0 \\ 0 \\ 0 \end{pmatrix} \quad (4)$$

Here, each vector on the right-hand side stands for a spectrum generated with the quoted set of

⁴Kaons are not separated from pions and are counted among the corresponding π -channels.

Background source	Event class		
	e-h	μ -h	e- μ
leptonic			
e-e	0.73 %	–	0.00 %
e- μ , μ -e	1.70 %	0.99 %	
μ - μ	–	1.64 %	0.12 %
hadronic			
h-h	0.72 %	1.55 %	–
e-h		–	1.73 %
h- μ	–		0.78 %
non- τ			
ee \rightarrow ee	0.06 %	–	0.00 %
ee \rightarrow $\mu\mu$	–	0.56 %	0.06 %
$\gamma\gamma \rightarrow$ ee	0.03 %	–	0.00 %
$\gamma\gamma \rightarrow$ $\mu\mu$	–	0.21 %	0.04 %
Total	3.3 %	5.0 %	2.8 %

Table 2

Background from misidentified τ decays, Bhabha, μ -pair and two-photon events. For simplicity the three hadronic channels have been summed up.

Michel parameters.

For a particular basis, the respective coefficients can be calculated by solving the equation system $\mathbf{q}_\ell = M_\ell \cdot \mathbf{c}_\ell$, where \mathbf{q}_ℓ is the vector $(1, \rho_\ell, \xi_\ell, \xi\delta_\ell, \eta_\ell)$, \mathbf{c}_ℓ is the vector of coefficients $(c_1, c_2, c_3, c_4, c_5)$, and M_ℓ is a 5×5 matrix given by:

$$M_\ell = \begin{pmatrix} 1 & 1 & 1 & 1 & 1 \\ \rho_{\ell 1} & \rho_{\ell 2} & \rho_{\ell 3} & \rho_{\ell 4} & \rho_{\ell 5} \\ \xi_{\ell 1} & \xi_{\ell 2} & \xi_{\ell 3} & \xi_{\ell 4} & \xi_{\ell 5} \\ \xi\delta_{\ell 1} & \xi\delta_{\ell 2} & \xi\delta_{\ell 3} & \xi\delta_{\ell 4} & \xi\delta_{\ell 5} \\ \eta_{\ell 1} & \eta_{\ell 2} & \eta_{\ell 3} & \eta_{\ell 4} & \eta_{\ell 5} \end{pmatrix}. \quad (5)$$

Here $\rho_{\ell 1}$ denotes the value of ρ_ℓ in the first basis spectrum, $\rho_{\ell 2}$ its value in the second spectrum and so forth. Hence, for given values of the Michel parameters the coefficients with respect to the basis M_ℓ are $\mathbf{c}_\ell = (M_\ell)^{-1} \cdot \mathbf{q}_\ell$. This allows one to fit the 4 Michel parameters to the data by adjusting the corresponding coefficients, i.e. the relative contributions of the basis spectra.

This method is also applicable to the correlation spectra, which can be represented by a composition that is bilinear in the 2×4 Michel parameters of the two τ decays (or of second order in the 4 parameters if the decays are identical)⁵. The correlation basis is the tensor product of two single decay bases. Now, 25 coefficients appear in the decomposition which are not all independent. They can again be calculated by inversion of the corresponding 25×25 matrix.

3.2. Monte Carlo simulated samples

The τ -pair Monte Carlo (MC) sample was generated using the KORALZ-3.8 generator and a modified version of the TAUOLA-1.5 decay library which was extended to include the full generalized matrix element [10]. Since finite MC samples are used to describe possibly small variations in the shape of the spectra, it is vital to keep statistical fluctuations as small as possible. To avoid gaussian smearing between corresponding bins of different basis spectra, each event is used for as many spectra as possible. An acceptance/rejection method is used where an event is flagged as accepted for each spectrum for which the generated random weight is below any of the predicted values (and not just the standard V-A) and it is rejected only if it belongs to none of the considered spectra. As a side effect, this makes the generation of the MC samples much more efficient.

3.3. Adjusted Likelihood

For every mixture of basis spectra, a likelihood is computed, assuming Poisson errors in each bin. Although the generated MC sample is about four times larger than the data sample, there are still bins with only few entries, typically in the correlation spectra in regions of high x . Therefore, fluctuations of both data and MC have been taken into account. To accomplish this, an adjusted likelihood is applied [11] by calculating in each bin i the most probable expectation with which data and MC are consistent:

$$\ln \mathcal{L}_i = (d_i \ln f_i - f_i) + \sum_{j=1}^{N_{\text{spectra}}} (a_{ji} \ln A_{ji} - A_{ji}). \quad (6)$$

⁵This is the case when e- μ universality is assumed.

Here d_i is the observed number of data events, N_{spectra} is the number of MC basis spectra (5 or 25), a_{ji} is the generated number of MC events in spectrum j and A_{ji} is the best estimator for the MC in the light of the data. The MC expectation $f_i = \sum_j p_j A_{ji}$ is the composition of the best estimators using the mixing coefficients p_j . The first term accounts for the agreement between the ideal composition and the data, the second term for the agreement between the ideal and the observed MC distribution. The likelihood $\ln \mathcal{L} = \sum_i \ln \mathcal{L}_i$ is maximized with respect to both p_j and A_{ji} .⁶ The generalization to the case of the double lepton spectra is straightforward as the two indices can formally be flattened to only one.

Since for the prepared MC spectra the entries a_{ji} are statistically correlated, it is necessary to rewrite the expectation by means of independent numbers. To this end, the spectra are sorted by increasing numbers of events in each individual bin, and the coefficients are recalculated in terms of the differences between the bins, which are by construction independent.

3.4. Constraint on the eta parameter

The Michel parameter η corresponds to a change in the partial decay width when it deviates from zero. To eliminate any dependence on the overall efficiency, MC predictions are normalized to the data. Due to the large correlation of η with the ρ parameter, this makes configurations possible where the spectral shape is changed only slightly while the value of η is inconsistent with the observed branching ratio.

Such a behavior is avoided by constraining the branching ratios to their measured values throughout the fit. In the general ansatz for the Lorentz structure, the leptonic width is in lowest order changed to:

$$\Gamma_\ell(\eta_\ell) = \Gamma_\ell^{(\text{SM})} \left(1 + 4\eta_\ell \frac{m_\ell}{m_\tau} \right). \quad (7)$$

From the measurement of the τ lifetime, τ_τ , the expected branching ratio, $B_\ell \equiv B(\tau \rightarrow \ell \nu_\ell \nu_\tau)$, can, depending on the value of η_ℓ , be calculated

⁶For each set of coefficients p_j the estimators A_{ji} can be calculated by solving an equation system.

as $B_\ell(\eta_\ell) = \Gamma_\ell(\eta_\ell) \tau_\tau$. This relation can be used to calculate the most probable value of η_ℓ :

$$\hat{\eta}_\ell = \frac{1}{4} \frac{m_\tau}{m_\ell} \left(\frac{B_\ell}{\Gamma_\ell^{(\text{SM})} \tau_\tau} - 1 \right). \quad (8)$$

Using the published OPAL results for the $\tau \rightarrow \mu \nu_\mu \nu_\tau$ branching ratio, $B_\mu = 0.1736 \pm 0.0027$ [12], and the τ lifetime, $\tau_\tau = (289.2 \pm 2.1)$ fs [13], one determines, $\hat{\eta}_\mu = 0.032 \pm 0.073$, which is consistent with zero. The constraint on η is applied by adding the following term to the log likelihood:

$$\ln \mathcal{L}_\ell^{\text{constraint}} = -\frac{1}{2} \frac{(\Gamma_\ell(\eta_\ell) \tau_\tau - B_\ell)^2}{(\Gamma_\ell(\eta_\ell) \Delta\tau_\tau)^2 + (\Delta B_\ell)^2}. \quad (9)$$

The use of this constraint makes the fit result for η_μ dominated by the branching ratio and lifetime measurements while the other parameters are still sensitive to the allowed variation in the η_μ -dependent part of the shape. It has to be noted that the constrained value of η_μ assumes total strength of the decay coupling to be universal.

4. RESULTS

The result of the global fit to single- e , single- μ and e - μ -correlations (figures 1, 2 and 3) with seven free parameters is shown in table 3. The covariance matrix can be found in [1].

4.1. Systematic errors

Various systematic uncertainties arising from detector specific and method inherent sources have been investigated. Uncertainties concerning the MC at the generator level, i.e., radiation effects, branching fractions, process kinematics etc., have been found to be negligible. The uncertainties in the absolute scale and the resolution of the energy and momentum measurements have been determined by comparing $e^+e^- \rightarrow e^+e^-$ and $e^+e^- \rightarrow \mu^+\mu^-$ events from data control samples with the corresponding MC events. The simulated MC efficiency has been compared to tagged Bhabha and μ -pair events covering the high x region as well as tagged two-photon events at low x . The ratio of the efficiencies in data and MC has been found to be consistent with unity,

$\tau \rightarrow e \nu_e \nu_\tau$	
ρ_e	$0.779 \pm 0.047 \pm 0.029$
ξ_e	$1.13 \pm 0.39 \pm 0.14$
$(\xi\delta)_e$	$0.72 \pm 0.31 \pm 0.14$
η_e	0 (fixed)
$\tau \rightarrow \mu \nu_\mu \nu_\tau$	
ρ_μ	$0.777 \pm 0.044 \pm 0.016$
ξ_μ	$0.79 \pm 0.41 \pm 0.05$
$(\xi\delta)_\mu$	$0.63 \pm 0.23 \pm 0.09$
η_μ	$0.010 \pm 0.065 \pm 0.001$

Table 3

Results of the global fit to the e-h, μ -h and e- μ energy spectra. The first error reflects both data and MC statistics, the second error is systematic.

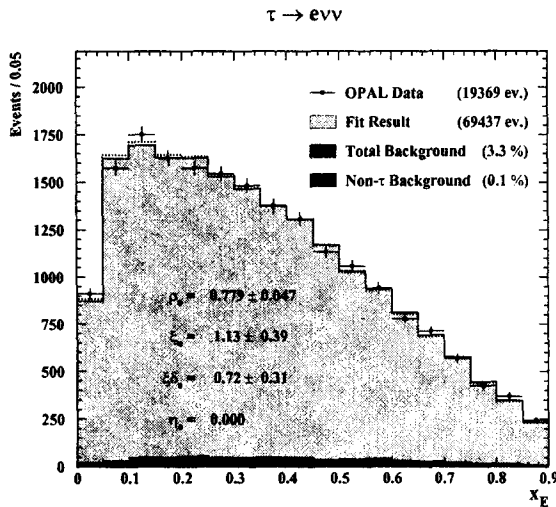


Figure 1. The spectrum of the scaled electron energy, x_E , from e-h events. The quoted Michel parameters are the subset from the global fit that determines the adjusted MC spectrum. The dotted line represents the SM expectation.

and has been varied within its error by weighting the MC events accordingly. Studies of the decay mode identification showed that the reference distributions of the likelihood variables agree

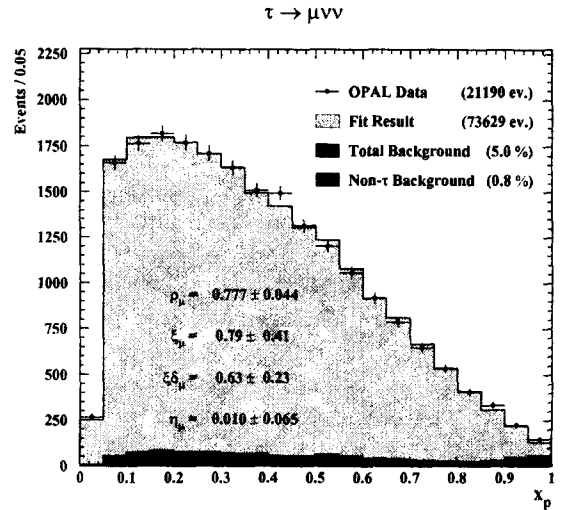


Figure 2. The spectrum of the scaled muon momentum, x_p , from μ -h events.

well with those of data samples that were tagged using other than the considered variable. Variation of the backgrounds from τ and non- τ sources had no significant impact on the fit result. Also, reducing the fit range by omitting the outer bins at low and high x shows no significant effect.

By using different sets of basis spectra it has been verified that the particular choice of the basis does not impose a bias. Due to the finite MC statistics some bases were less sensitive to the Michel parameters than the preferred one, however, all alternative fits were consistent within their errors.

4.2. Lepton universality

With the assumption of universality between electron and muon, i.e., with all couplings $g_{e\omega}^\gamma$ being the same for $\tau \rightarrow e \nu_e \nu_\tau$ and $\tau \rightarrow \mu \nu_\mu \nu_\tau$, one set of Michel parameters can be used to describe both leptonic decays. The fit then yields the results in table 4. The covariance matrix is quoted in [1].

4.3. Mass of a charged Higgs boson

In models with two scalar field doublets, such as the Minimal Supersymmetric Standard Model (MSSM), a charged Higgs boson exists which con-

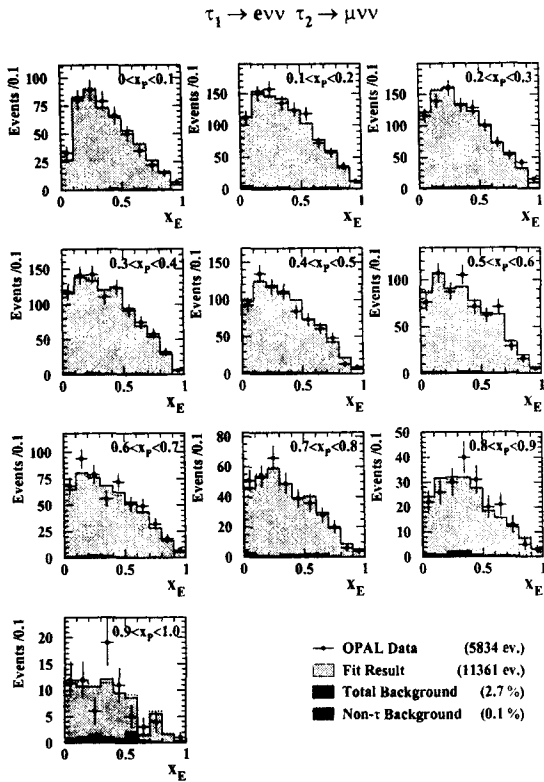


Figure 3. The correlated decay spectra from $e-\mu$ events together with the adjusted MC spectrum from the global fit. The distribution of the scaled energy, x_E , of the decay electron is shown in slices for each bin of the scaled muon momentum, x_p .

$\tau \rightarrow \ell \nu_\ell \nu_\tau$	
ρ	$0.781 \pm 0.028 \pm 0.018$
ξ	$0.98 \pm 0.22 \pm 0.10$
$\xi\delta$	$0.65 \pm 0.14 \pm 0.07$
η	$0.027 \pm 0.055 \pm 0.005$

Table 4

Result of the $e-\mu$ universality fit.

tributes to the τ decay through a scalar coupling. The value of the additional coupling is, assuming

vanishing neutrino masses [14]:

$$g_\ell^S = -m_\ell m_\tau \left(\frac{\tan \beta}{m_{H^\pm}} \right)^2, \quad (10)$$

where m_{H^\pm} is the mass of the charged Higgs boson and $\tan \beta$ is the ratio of the vacuum expectation values of the two Higgs doublets. Under the assumption that the neutrinos are still left-handed, the couplings are of the type g_{RR}^S . After applying the normalization $N_\ell = |g_{LL}^V|^2 + \frac{1}{4}|g_{RR,\ell}^S|^2$, the Michel parameters can be written as:

$$\rho_\ell = \frac{3}{4}, \quad \xi_\ell = \frac{1 - (g_{RR,\ell}^S/2)^2}{1 + (g_{RR,\ell}^S/2)^2}, \quad (11)$$

$$(\xi\delta)_\ell = \frac{3}{4}\xi_\ell, \quad \eta_\ell = -\frac{g_{RR,\ell}^S/2}{1 + (g_{RR,\ell}^S/2)^2}.$$

Using these relations, the value of $m_{H^\pm}/\tan \beta$ can be fitted directly to the data. The likelihood function saturates for high Higgs boson masses or small values of $\tan \beta$. From the log likelihood a limit can be extracted as:

$$m_{H^\pm} > 0.97 \times \tan \beta \text{ GeV} \quad (95\% \text{ C.L.}). \quad (12)$$

4.4. Left-right symmetric model

In left-right symmetric models, parity violation of the charged current is caused by spontaneous symmetry breaking. In such models a second W boson is assumed [15]. The mass eigenstates $W_{1,2}$ are not necessarily identical to the weak eigenstates $W_{L,R}$ as mixing can occur. The model is parameterized by the mass ratio of the physical eigenstates, $\beta = m_{W_1}^2/m_{W_2}^2$, and by the mixing angle ζ which connects the physical masses to the masses of the weak eigenstates:

$$m_{W_{1,2}}^2 = \frac{1}{2} \left(m_{W_L}^2 + m_{W_R}^2 \pm \frac{m_{W_L}^2 - m_{W_R}^2}{\cos 2\zeta} \right). \quad (13)$$

In this model the Michel parameters can be written as:

$$\rho = \frac{3}{4} \cos^4 \zeta \left(1 + \tan^4 \zeta + \frac{4\beta}{1 + \beta^2} \tan^2 \zeta \right),$$

$$\xi = \cos^2 \zeta (1 - \tan^2 \zeta) \frac{1 - \beta^2}{1 + \beta^2}, \quad (14)$$

$$\xi\delta = \frac{3}{4}\xi, \quad \eta = 0.$$

A limit on β can be transformed into a limit on m_{W_2} by using the direct measurement of the W mass: $m_{W_1} = (80.43 \pm 0.08) \text{ GeV}$ [7]. Integration of the two-dimensional likelihood over ζ yields a function from which a limit on m_{W_2} , valid for arbitrary mixing, can be extracted as:

$$m_{W_2} > 137 \text{ GeV} \quad (95 \% \text{ C.L.}). \quad (15)$$

Similarly, integration over m_{W_2} allows one to set bounds on the mixing angle independently of the W_2 mass:

$$|\zeta| < 0.12 \quad (95 \% \text{ C.L.}). \quad (16)$$

For $\zeta = 0$, W_2 and W_R become identical, and a limit on m_{W_R} can be given from a fit of the Michel parameter ξ alone. In this case there is no mixing but an additional coupling to a pure right-handed W that is proportional to its inverse mass, $g_{LL,RR}^V \sim 1/m_{W_{L,R}}$. Under the assumption of no mixing one obtains:

$$m_{W_R} > 145 \text{ GeV} \quad (95 \% \text{ C.L.}). \quad (17)$$

4.5. Limits on the couplings

From the measurement of the Michel parameters, limits on the absolute values of the couplings $g_{e\nu}^\gamma$ can be calculated. This is done by constructing positive-semidefinite expressions and inserting the measured parameters. A general approach to find such expressions is to follow the boundaries of the physically allowed parameter space.

From the definition of the Michel parameters it is obvious that they cannot vary independently over their full definition range. To clarify their interdependence it is very instructive to write them in the notation [16]:⁷

$$\begin{aligned} \rho &= \frac{3}{4}(\beta^+ + \beta^-) + (\gamma^+ + \gamma^-) \\ \xi &= 3(\alpha^- - \alpha^+) + (\beta^- - \beta^+) + \frac{7}{3}(\gamma^+ - \gamma^-) \\ \xi\delta &= \frac{3}{4}(\beta^- - \beta^+) + (\gamma^+ - \gamma^-), \end{aligned} \quad (18)$$

where

$$\begin{aligned} \alpha^+ &= |g_{RL}^V|^2 + \frac{1}{16}|g_{RL}^S + 6g_{RL}^T|^2 \\ \alpha^- &= |g_{LR}^V|^2 + \frac{1}{16}|g_{LR}^S + 6g_{LR}^T|^2 \end{aligned} \quad (19)$$

⁷The parameter η is not regarded here because it is not used for this kind of limits.

$$\begin{aligned} \beta^+ &= |g_{RR}^V|^2 + \frac{1}{4}|g_{RR}^S|^2 & \gamma^+ &= \frac{3}{16}|g_{RL}^S - 2g_{RL}^T|^2 \\ \beta^- &= |g_{LL}^V|^2 + \frac{1}{4}|g_{LL}^S|^2 & \gamma^- &= \frac{3}{16}|g_{LR}^S - 2g_{LR}^T|^2 \end{aligned}$$

The normalization is then given by:

$$\alpha^+ + \alpha^- + \beta^+ + \beta^- + \gamma^+ + \gamma^- = 1. \quad (20)$$

This shows that the three Michel parameters ρ , ξ and $\xi\delta$ depend only on the six positive real numbers $0 \leq \alpha^\pm, \beta^\pm, \gamma^\pm \leq 1$. With this simplification one can directly read from equation 18 the physical ranges as:

$$0 \leq \rho \leq 1, \quad -3 \leq \xi \leq 3, \quad -1 \leq \xi\delta \leq 1. \quad (21)$$

By setting α^\pm , β^\pm and γ^\pm to their extreme values one finds the six points:

	A^+	A^-	B^+	B^-	C^+	C^-
ρ	0	0	3/4	3/4	1	1
ξ	-3	3	-1	1	7/3	-7/3
$\xi\delta$	0	0	-3/4	3/4	1	-1

One of them, B^- , corresponds to the SM. The points B^\pm lie on the segments between the other two points: $B^\pm = \frac{3}{4}(C^\mp - A^\mp)$. Thus, only four points span the entire parameter space with an illustrative geometrical interpretation: the physically allowed region of the three Michel parameters $(\rho, \xi, \xi\delta)$ forms a tetrahedron (figure 4).

The idea to get constraints for the parameter sets $(\rho, \xi, \xi\delta)$ is to formulate boundary conditions which the points inside the tetrahedron fulfill. The simplest expression comes from the requirement that the point lies in the cube surrounding the tetrahedron:⁸

$$1 - \rho \geq 0. \quad (22)$$

More stringent conditions follow from the faces of the tetrahedron itself. Apparently, one of the edges, between A^+ and A^- , falls on the ξ -axis. This and the other two edges starting at the point A^+ are represented by the vectors:

$$\mathbf{a} = \begin{pmatrix} 0 \\ 6 \\ 0 \end{pmatrix}, \quad \mathbf{b} = \begin{pmatrix} 1 \\ 16/3 \\ 1 \end{pmatrix}, \quad \mathbf{c} = \begin{pmatrix} 1 \\ 2/3 \\ -1 \end{pmatrix} \quad (23)$$

⁸Similar expressions for the other Michel parameters, $3 - \xi$ and $1 - \xi\delta$, have much smaller sensitivity than the combined ones derived in this section.

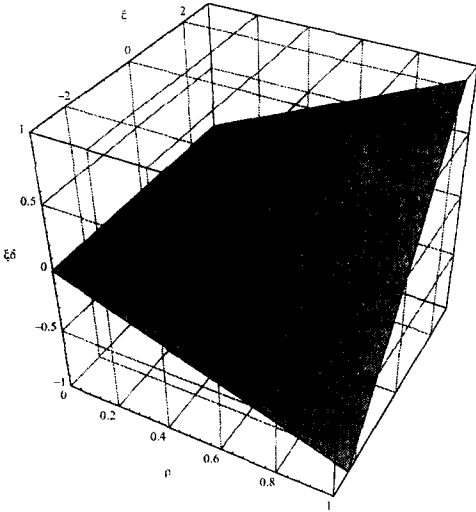


Figure 4. The tetrahedron representing the physically allowed Michel parameter space for $(\rho, \xi, \xi\delta)$. The SM prediction lies on one of the edges as indicated by the black dot.

Vectors that are perpendicular to the faces opposite to the points C^- and A^- and that point inside the tetrahedron can be constructed from the cross products of the edges, $\mathbf{n}_{C^-} \equiv \mathbf{a} \times \mathbf{b}$ and $\mathbf{n}_{A^-} \equiv \mathbf{b} \times \mathbf{c}$, respectively:

$$\mathbf{n}_{C^-} = \begin{pmatrix} 6 \\ 0 \\ -6 \end{pmatrix}, \quad \mathbf{n}_{A^-} = \begin{pmatrix} -6 \\ 2 \\ -14/3 \end{pmatrix}. \quad (24)$$

The distance of a point inside the tetrahedron from the C^- face can be written as:

$$d_{C^-} = \begin{pmatrix} \rho \\ \xi \\ \xi\delta \end{pmatrix} \cdot \begin{pmatrix} 1 \\ 0 \\ -1 \end{pmatrix} = \rho - \xi\delta \geq 0. \quad (25)$$

The distance from the A^- face can be written as:

$$d_{A^-} = \left[\begin{pmatrix} \rho \\ \xi \\ \xi\delta \end{pmatrix} - \begin{pmatrix} 0 \\ -3 \\ 0 \end{pmatrix} \right] \cdot \begin{pmatrix} -1 \\ 1/3 \\ -7/9 \end{pmatrix} \\ = 1 - \rho + \frac{1}{3}\xi - \frac{7}{9}\xi\delta \geq 0. \quad (26)$$

The edge between the two faces is the intersection of the above planes ($d_{C^-} = d_{A^-}$) from which

follows:

$$\frac{1}{2} - \rho + \frac{1}{6}\xi + \frac{1}{9}\xi\delta = 0. \quad (27)$$

Inserting the SM values shows that the V–A prediction lies on this edge. This is the reason why the two faces lead to the strongest limits on the couplings. The sum of the distances from the two faces is another positive quantity:

$$d_{C^-} + d_{A^-} = 1 + \frac{1}{3}\xi + \frac{16}{9}\xi\delta \geq 0. \quad (28)$$

It is remarkable that this expression, normalized to its maximal value of 2, i.e. the average distance from the two faces, can be interpreted as the probability that the τ lepton decays as a right-handed particle (see below).

Inserting the relations in equation 18 into the above expressions yields:

$$1 - \rho = \alpha^+ + \alpha^- + \frac{1}{4}(\beta^+ + \beta^-), \\ \rho - \xi\delta = \frac{3}{2}\beta^+ + 2\gamma^-, \quad (29)$$

$$1 - \rho + \frac{1}{3}\xi - \frac{7}{9}\xi\delta = 2\alpha^- + \frac{1}{2}\beta^+, \\ \frac{1}{2}(1 + \frac{1}{3}\xi - \frac{16}{9}\xi\delta) = \alpha^- + \beta^+ + \gamma^-,$$

which verifies that all expressions are positive quantities. Thus, upper limits on any of the expressions can be translated into upper limits on some of the coupling constants $g_{e\omega}^\gamma$.

The correlation between either two of the Michel parameters $(\rho, \xi, \xi\delta)$ can be interpreted in the two-dimensional projections of the tetrahedron shown in figure 5. The three plots in figure 6 show the result of the $e\text{-}\mu$ universality fit in these projections of the Michel parameter space.

4.6. Limits on the couplings

The explicit dependence of the quoted expressions on the couplings is:

$$1 - \rho = \frac{1}{4}|g_{LL}^V|^2 + |g_{LR}^V|^2 + |g_{RL}^V|^2 + \frac{1}{4}|g_{RR}^V|^2 \\ + \frac{1}{16}|g_{LL}^S|^2 + \frac{1}{16}|g_{RR}^S|^2 \quad (30) \\ + \frac{1}{16}|g_{LR}^S|^2 + 6g_{LR}^T|^2 + \frac{1}{16}|g_{RL}^S|^2 + 6g_{RL}^T|^2$$

$$\rho - \xi\delta = \frac{3}{2}|g_{RR}^V|^2 + \frac{3}{8}|g_{LR}^S|^2 - 2g_{LR}^T|^2 + \frac{3}{8}|g_{RR}^S|^2 \quad (31)$$

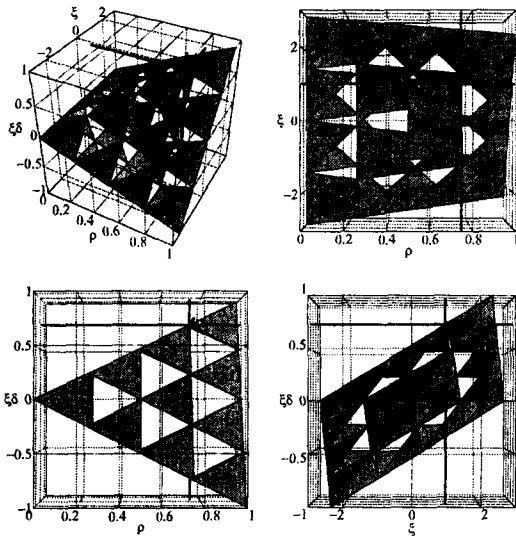


Figure 5. Three projections of the $(\rho, \xi, \xi\delta)$ tetrahedron representing the physically allowed Michel parameter space.

$$1 - \rho + \frac{1}{3} \xi - \frac{7}{9} \xi\delta = |g_{LR}^V|^2 + \frac{1}{4} |g_{RR}^V|^2 + \frac{1}{16} |g_{LR}^S|^2 + 6 |g_{LR}^T|^2 + \frac{1}{16} |g_{RR}^S|^2 \quad (32)$$

An upper bound on $|g_{RL}^V|$ as well as weak upper bounds on $|g_{RL}^S|$ and $|g_{RL}^T|$ can be set from the expression $1 - \rho$. Limits on $|g_{RR}^V|$ and $|g_{RR}^S|$ can be retrieved from the expression $\rho - \xi\delta$. Limits on the remaining couplings $|g_{LR}^S|$ and $|g_{LR}^T|$ follow from the probability Q_R which is given below. An even stronger limit on $|g_{LR}^V|$ can be set from the 3-dimensional expression $1 - \rho + \frac{1}{3} \xi - \frac{7}{9} \xi\delta$. Only the coupling $|g_{LL}^S|$ cannot be constrained since it cannot be distinguished from the SM coupling $|g_{LL}^V|$ on basis of the four Michel parameters.

The probability that the τ lepton decays as a right-handed particle can be calculated as the normalized sum of all couplings of the type g_{eR}^7 :

$$Q_R = \frac{1}{4} |g_{LR}^S|^2 + \frac{1}{4} |g_{RR}^S|^2 + |g_{LR}^V|^2 + |g_{RR}^V|^2 + 3 |g_{LR}^T|^2 = \frac{1}{2} (1 + \frac{1}{3} \xi - \frac{16}{9} \xi\delta). \quad (33)$$

Using the correlations between the parameters the $e-\mu$ universality fit yields:

$$Q_R = 0.089 \pm 0.131 < 0.304 \quad (90\% \text{ C.L.}). \quad (34)$$

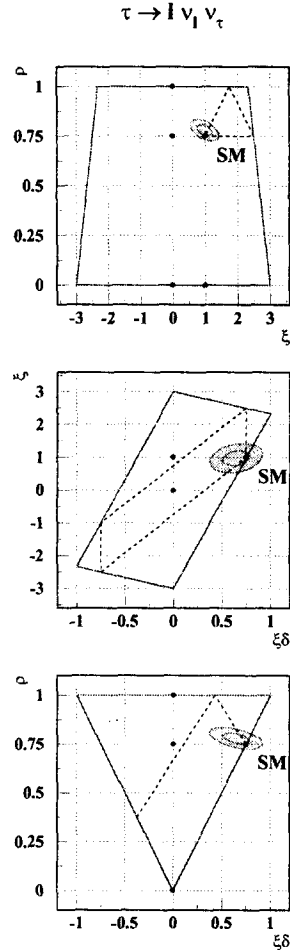


Figure 6. 1 and 2 σ ellipses of the $e-\mu$ universality fit in the 2-dimensional projections of the Michel parameter space. The solid line encloses the physically allowed region, the dashed line confines the area that remains when the third parameter is fixed to its SM value. The closed circles indicate the basis spectra used in the fit.

From the result of the global and the $e-\mu$ universality fit, the bounds given in table 5 can be set at the 90% confidence level. Figure 7 shows the limits on the universal coupling constants normalized to their maximum values.

5. CONCLUSION

The measurement of the Michel parameters remains an important task in order to probe the

	$\tau \rightarrow e\nu_e\nu_\tau$	$\tau \rightarrow \mu\nu_\mu\nu_\tau$	$\tau \rightarrow \ell\nu_\ell\nu_\tau$
$ g_{RR}^S $	< 1.36	< 1.25	< 1.05
$ g_{LR}^S $	< 1.40	< 1.27	< 1.10
$ g_{RL}^S $	< 2.00	< 2.00	< 2.00
$ g_{LL}^S $	≤ 2	≤ 2	≤ 2
$ g_{RR}^V $	< 0.68	< 0.62	< 0.53
$ g_{LR}^V $	< 0.43	< 0.39	< 0.35
$ g_{RL}^V $	< 0.56	< 0.55	< 0.52
$ g_{LL}^V $	≤ 1	≤ 1	≤ 1
$ g_{LR}^T $	< 0.41	< 0.37	< 0.32
$ g_{RL}^T $	< 0.52	< 0.52	< 0.51

Table 5
90 % confidence limits on the coupling constants with and without the assumption of e-μ universality. No limits can be set on g_{LL}^S and g_{LL}^V which are listed for completeness.

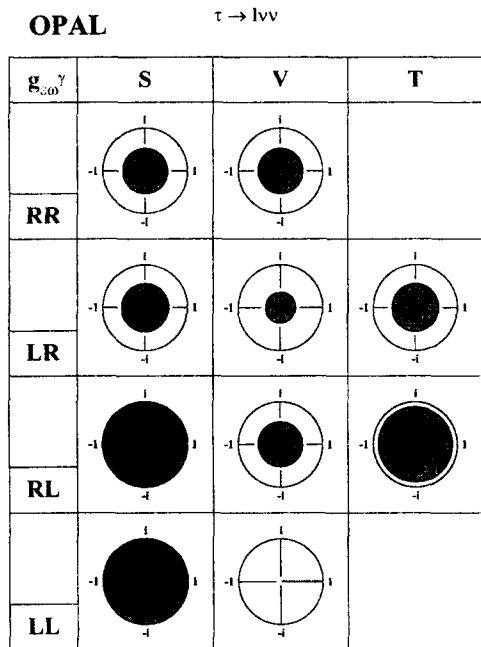


Figure 7. 90 % confidence limits on the normalized coupling constants, $g_{e\omega}^S/2$, $g_{e\omega}^V$, and $g_{e\omega}^T/\sqrt{3}$, under the assumption of e-μ universality.

Lorentz structure of the charged weak current. Many extensions to the V–A theory would show up as changes in the shape of the lepton decay spectra. The investigation of the τ decay spectra provides an interesting window for non-standard couplings and new intermediate bosons. Limits on new effects can be obtained from the interpretation of the Michel parameters with respect to their physically allowed region. Although recent measurements have drastically reduced the available parameter space, current limits on the couplings leave still room for new physics to hide. It can be expected that high-luminosity experiments at the B-factories and at a future τ -charm factory will either further push down these limits - or reveal a hint for new physics.

REFERENCES

1. K. Ackerstaff *et al.*, CERN Report No. EP-98-104, 1998 (unpublished).
2. A. Pich and J. P. Silva, Phys. Rev. **D52**, 4006 (1995).
3. L. Michel, Proc. Phys. Soc. **A63**, 514 (1950).
4. C. Bouchiat and L. Michel, Phys. Rev. **106**, 170 (1957).
5. C. A. Nelson, Phys. Rev. **D40**, 123 (1989).
6. W. Fetscher, Phys. Rev. **D42**, 1544 (1990).
7. D. Abbaneo *et al.*, CERN Report No. PPE-97-154, 1997 (unpublished).
8. OPAL, G. Alexander *et al.*, Z. Phys. **C72**, 365 (1996).
9. OPAL, K. Ahmet *et al.*, Nucl. Instrum. Meth. **A305**, 275 (1991).
10. M. Schmidtler, Karlsruhe U., IEKP Report No. KA-93-14, 1993 (unpublished).
11. R. Barlow and C. Beeston, Comput. Phys. Commun. **77**, 219 (1993).
12. OPAL, G. Alexander *et al.*, Phys. Lett. **B374**, 341 (1996).
13. OPAL, R. Akers *et al.*, Z. Phys. **C66**, 543 (1995).
14. H. E. Haber, SLAC Report No. SLAC-0343, 1989 (unpublished).
15. J. Polak and M. Zralek, Nucl. Phys. **B363**, 385 (1991).
16. A. Rougé, Ecole Polytechnique Report No. X-LPNHE-95-01, 1995 (unpublished).